 CMC, vol.28, no.2, pp.147-164, 2012

3D Analysis of the Forced Vibration of a Prestressed Rectangular Composite Plate With Two Neighboring Cylindrical Cavities

S.D. Akbarov[1,2], N. Yahnioglu[3] and U. Babuscu Yesil[3]

Abstract: This paper presents an analysis of the forced vibration of an initially stressed rectangular composite plate containing two neighboring cylindrical cavities. The initial stresses are caused by stretching or compressing of the plate with uniformly distributed normal static forces acting on the two opposite end-planes which are parallel to the central axes of the aforementioned cylindrical cavities. The influence of the initial stresses on the stress concentration around the cavities caused by the additional uniformly distributed time harmonic forces acting on the upper face plane of the plate are given. The considered problem is formulated within the framework of the Three-Dimensional Linearized Theory of Elastic Waves in Initially Stressed Bodies. For the solution to this problem 3D FEM is employed. The numerical results on the influence of the initial stresses on the stress concentration around the cavities, as well as on the fundamental frequencies of the plate are presented and discussed.

Keywords: Initial stress, forced vibration, cylindrical cavity, 3D FEM, rectangular plate, composite.

1 Introduction

In many engineering applications, such as the aerospace, underwater and automotive industries, frequent mechanical problems due to cutouts in the form of cavities are inevitable. The presence of cavities in structural elements leads to undesired stress or strain concentrations around these cavities. Hence, the cavities may reduce the working ability of the structural elements contained around these cavi-

[1] Yildiz Technical University, Faculty of Mechanical Engineering, Department of Mechanical Engineering, Yildiz Campus, 34349, Besiktas, Istanbul-Turkey.

[2] Institute of Mathematics and Mechanics of National Academy of Sciences of Azerbaijan, 37041, Baku- Azerbaijan

[3] Yildiz Technical University, Faculty of Chemistry and Metallurgy, Department of Mathematical Engineering, Davutpasa Campus,34210, Istanbul-Turkey.

ties. Therefore, knowledge of the stress concentration is of particular interest and has been a subject of many investigations such as Chaudhuri (2007), Chernopiskii (2009), Savin (1961), Toubal, Karama and Lorrai (2005), Zhen and Wanji (2009), Zheng, Chang-Boo, Chongdu and Hyeon (2008) and many others listed in these references. Moreover, the existence of such cavities in the structural elements may significantly change their dynamical characteristics, such as their natural frequencies (Kwaka and Han (2007), Sivakumar and Iyengar (1999) and Zamanov (1999)). Therefore investigations of the forced vibration of the plates with cavities have significance not only in relation to knowledge of the stress concentration, but also in relation to the study of these cavities on the natural frequencies of the structural elements. Moreover, another significant fact which has been investigated by Akbarov, Yahnioglu and Babuscu Yesil (2008, 2010), Akbarov, Yahnioglu and Yucel (2004), Babuscu Yesil (2010), Khoma and Kondratenko (2008), Yahnioglu (2007) and Yahnioglu and Babuscu Yesil (2009),is the influence of the initial stresses on the abovementioned stress concentration and natural frequencies. Initial stresses in elements of construction may arise as a result of the change in environmental conditions such as changing temperature or in the welding process etc. Moreover, the stresses arising with working forces can also be taken as the initial stresses with respect to the additional stresses caused by earthquakes or other similar forces. Consequently, investigations of the forced vibration of initially stressed structural elements containing holes (2D problems) and cavities (3D problems) have theoretical and practical significance. However, up to now there has only been one investigation (Akbarov, Yahnioglu and Babuscu Yesil (2010)) in this field and this investigation relates to the forced vibration of the composite rectangular plate containing a cylindrical cavity with rectangular cross section with rounded corners. The present paper extends this investigation for the case where the rectangular plate contains two parallel neighboring cylindrical cavities with the same rectangular cross sections with rounded corners. It is assumed that this plate is loaded initially by uniformly distributed normal static forces acting on two opposite end-planes which are parallel to the cavities' central axes and that time-harmonic normal forces act on the upper face plane of the plate. The initial stresses caused by the initial loading noted above are determined within the scope of the classical linear theory of elasticity. Investigation of these initial stresses on the stress concentration and natural frequencies of the plate is carried out by the use of the Three-Dimensional Linearized Theory of Elastic Waves in Initially Stressed Bodies (TDLTEWISB) (Guz (2004)). The corresponding boundary-value problem is solved by employing 3D FEM. The numerical results on the influence of the initial stresses and on the influence of the interaction between the cavities on the stress concentration caused by the additional time-harmonic loading are presented and discussed.

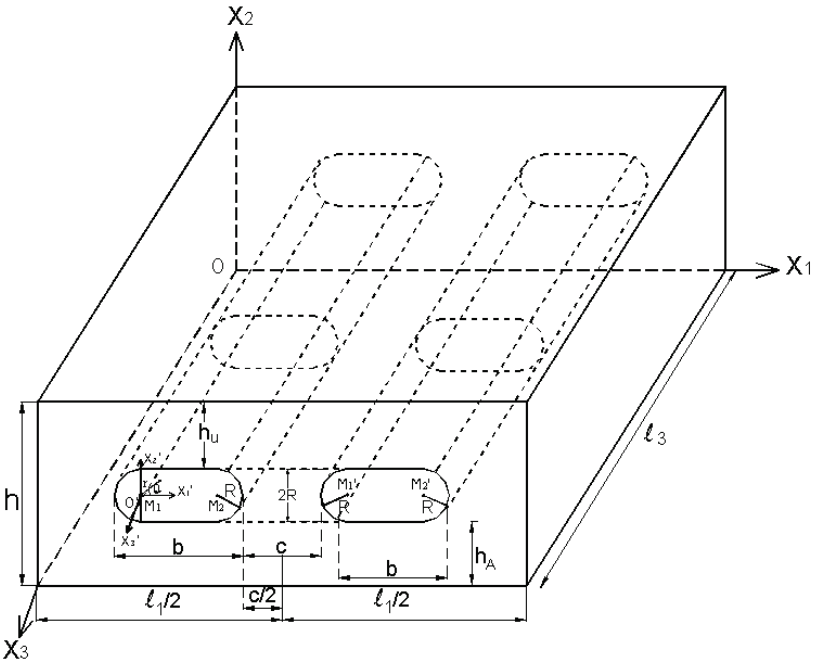

Figure 1: The geometry of the considered rectangular plate

2 Formulation of the problem

This study considers a rectangular plate containing two neighboring parallel cylindrical holes whose cross sections are rectangular with rounded-off corners. Its geometry is shown in Fig 1. The Cartesian coordinate system $Ox_1x_2x_3$ is associated with the plate so as to give Lagrange coordinates in the initial state. Assume that the plate occupies the region:

$$\Omega' = (\Omega - \Omega_I - \Omega_{II}) \tag{1}$$

where,

$$\Omega = \{0 \le x_1 \le \ell_1; 0 \le x_2 \le h; 0 \le x_3 \le \ell_3\},$$

$$\Omega_I = \{x_{01} \le x_1 \le (x_{01} + b - 2R); y_{01} - R \le x_2 \le y_{01} + R; 0 \le x_3 \le \ell_3\} \cup$$

$$\left\{(x_1,x_2,x_3)\left|\begin{array}{l}(x_1-x_{01})^2+(x_2-y_{01})^2\le R^2,\\ (x_{01}-R)\le x_1\le x_{01};\\ y_{01}-R\le x_2\le y_{01}+R;\\ 0\le x_3\le \ell_3\end{array}\right.\right\}\cup$$

$$\left\{(x_1,x_2,x_3)\left|\begin{array}{l}(x_1-x_{02})^2+(x_2-y_{02})^2\le R^2,\\ x_{02}\le x_1\le x_{02}+R;\\ y_{01}-R\le x_2\le y_{01}+R\end{array}\right.\right\}$$

$$\Omega_{II}=\left\{x'_{01}\le x_1\le\left(x'_{01}+b-2R\right);\, y'_{01}-R\le x_2\le y'_{01}+R;\, 0\le x_3\le\ell_3\right\}\cup$$

$$\left\{\begin{array}{l}(x_1,x_2,x_3)|\,(x_1-x'_{01})^2+(x_2-y'_{01})^2\le R^2,\\ (x'_{01}-R)\le x_1\le x'_{01};\\ y'_{01}-R\le x_2\le y'_{01}+R;\\ 0\le x_3\le\ell_3\end{array}\right\}\cup$$

$$\left\{(x_1,x_2,x_3)\left|\begin{array}{l}(x_1-x'_{02})^2+(x_2-y'_{02})^2\le R^2,\\ x'_{02}\le x_1\le(x'_{02}+R);\\ y'_{01}-R\le x_2\le y'_{01}+R;\\ 0\le x_3\le\ell_3\end{array}\right.\right\} \tag{2}$$

In (2) (x_{01},y_{01}) $((x_{02},y_{02}))$ is the center of the left (right) half circular arc of the first hole near the left side of the plate and (x'_{01},y'_{01}) $((x'_{02},y'_{02}))$ is the center of the left (right) half circular arc of the second hole near the right side of the plate in the plane where x_3=const. It is assumed that the plate material is an orthotropic one with elastic symmetry axes Ox_1,Ox_2 andOx_3.

The solution procedure of the considered problem has two stages. In the first stage (initial state), the initial stress-state of the rectangular plate subjected to the uniformly distributed normal static forces q acting on two opposite end-planes which are parallel to the cavities' central axes is determined. In the second stage (perturbed state), the influence of the initial stresses on the stress concentrations around the cavities of the plate under the corresponding forced vibration of the initial stressed plate which is subjected to additional uniformly distributed dynamic (time-harmonic) normal forces with amplitude $p(<q)$ is determined. Henceforth all quantities referring to the initial state will be labeled by the superscript (0) and the repeated indices in equations are summed over their ranges.

According to the above, the initial stress-state can be determined by solving the boundary-value problem:

$$\frac{\partial\sigma_{ij}^{(0)}}{\partial xj}=0;\quad \boldsymbol{\sigma}^{(0)}=\mathbf{D}\boldsymbol{\varepsilon}^{(0)};\quad \varepsilon_{ij}^{(0)}=\frac{1}{2}\left(\frac{\partial u_i^{(0)}}{\partial x_j}+\frac{\partial u_j^{(0)}}{\partial x_i}\right) \tag{3}$$

$$u_2^{(0)}\Big|_{x_1=0;\ell_1} = u_2^{(0)}\Big|_{x_3=0;\ell_3} = 0, \quad \sigma_{1i}^{(0)}\Big|_{x_1=0;\ell_1} = q\delta_1^i, \quad \sigma_{2i}^{(0)}\Big|_{x_2=0;h} = 0,$$

$$\sigma_{31}^{(0)}\Big|_{x_3=0;\ell_3} = \sigma_{33}^{(0)}\Big|_{x_3=0;\ell_3} = 0, \quad \sigma_{ij}^{(0)} n_j^{(I)}\Big|_{S_I} = 0, \quad \sigma_{ij}^{(0)} n_j^{(II)}\Big|_{S_{II}} = 0 \; i;j = 1,2,3. \tag{4}$$

In equation (3) $\boldsymbol{\sigma}^{(0)}$, $\varepsilon^{(0)}$ and matrix $\mathbf{D}$ are determined as follows:

$$\left(\boldsymbol{\sigma}^{(0)}\right)^T = \left(\sigma_{11}^{(0)}\ \sigma_{22}^{(0)}\ \sigma_{33}^{(0)}\ \sigma_{23}^{(0)}\ \sigma_{13}^{(0)}\ \sigma_{12}^{(0)}\right), \quad \left(\varepsilon^{(0)}\right)^T = \left(\varepsilon_{11}^{(0)}\ \varepsilon_{22}^{(0)}\ \varepsilon_{33}^{(0)}\ \varepsilon_{23}^{(0)}\ \varepsilon_{13}^{(0)}\ \varepsilon_{12}^{(0)}\right)$$

$$\mathbf{D} = \begin{Bmatrix} A_{11} & A_{12} & A_{13} & 0 & 0 & 0 \\ A_{12} & A_{22} & A_{23} & 0 & 0 & 0 \\ A_{13} & A_{23} & A_{33} & 0 & 0 & 0 \\ 0 & 0 & 0 & 2A_{44} & 0 & 0 \\ 0 & 0 & 0 & 0 & 2A_{55} & 0 \\ 0 & 0 & 0 & 0 & 0 & 2A_{66} \end{Bmatrix}. \tag{5}$$

Moreover, in (4) S_I (S_{II}) shows the surface of the first (the second) cylindrical cavity and $n_j^{(I)}(n_j^{(II)})$ are the components of the unit's outward normal vector to the surface S_I (S_{II}).

To determine the stress-state caused by additional dynamic loading, the following boundary-value problem must be solved.

According to the TDLTEWISB (see Guz, (2004)), the following field equations:

$$\frac{\partial}{\partial x_j}\left(\sigma_{ji} + \sigma_{in}^{(0)}\frac{\partial u_i}{\partial x_n}\right) = \rho\frac{\partial^2 u_i}{\partial t^2}, \tag{6}$$

$$\boldsymbol{\sigma} = \mathbf{D}\boldsymbol{\varepsilon}; \quad \varepsilon_{ij} = \frac{1}{2}\left(\frac{\partial u_i}{\partial x_j} + \frac{\partial u_j}{\partial x_i}\right) \tag{7}$$

and boundary conditions:

$$u_2|_{x_1=0;\ell_1} = u_2|_{x_3=0;\ell_3} = 0,$$

$$\left(\sigma_{j1} + \sigma_{1n}^{(0)}\frac{\partial u_1}{\partial x_n}\right)n_j\Big|_{x_1=0;\ell_1} = \left(\sigma_{j3} + \sigma_{3n}^{(0)}\frac{\partial u_3}{\partial x_n}\right)n_j\Big|_{x_1=0;\ell_1} = 0,$$

$$\left(\sigma_{jk}+\sigma_{kn}^{(0)}\frac{\partial u_k}{\partial x_n}\right)n_j\Big|_{x_2=h}=pe^{i\omega t},$$

$$\left(\sigma_{ji}+\sigma_{in}^{(0)}\frac{\partial u_i}{\partial x_n}\right)n_j\Big|_{x_2=0}=0,$$

$$\left(\sigma_{j1}+\sigma_{1n}^{(0)}\frac{\partial u_1}{\partial x_n}\right)n_j\Big|_{x_3=0;\ell_3}=\left(\sigma_{j3}+\sigma_{3n}^{(0)}\frac{\partial u_3}{\partial x_n}\right)n_j\Big|_{x_3=0;\ell_3}=0,$$

$$\left(\sigma_{ji}+\sigma_{in}^{(0)}\frac{\partial u_i}{\partial x_n}\right)n_j^{(I)}\Big|_{S_I}=0,$$

$$\left(\sigma_{ji}+\sigma_{in}^{(0)}\frac{\partial u_i}{\partial x_n}\right)n_j^{(II)}\Big|_{S_{II}}=0,\quad i;j=1,2,3. \tag{8}$$

are satisfied. In (6)-(8) conventional notation is used and in equation (6) t is the time and ρ is the density of the plate material. Note that the equations and relations given in (6)-(8) coincide with the corresponding ones of the TDLTEWISB (Guz (2004)).

For the solution to the boundary value problem (6)-(8) the sought quantities are presented as follows:

$$\left\{\sigma_{ij},\varepsilon_{ij},u_i\right\}=\left\{\bar{\sigma}_{ij},\bar{\varepsilon}_{ij},\bar{u}_i\right\}\exp\left(i\omega t\right) \tag{9}$$

where $\bar{\sigma}_{ij},\bar{\varepsilon}_{ij}$ and $\bar{u}_i$ are the amplitude of the corresponding quantities. Using Eq. (9) in Eq. (6) and with some manipulations, the following equation in terms of the amplitude of the corresponding quantities is obtained:

$$\frac{\partial}{\partial x_j}\left(\bar{\sigma}_{ji}+\sigma_{in}^{(0)}\frac{\partial \bar{u}_i}{\partial x_n}\right)+\rho\omega^2\bar{u}_i=0. \tag{10}$$

Relation (7) and the boundary conditions in (8), except for the condition at $x_2=h$ given in Eq. (8), are identically satisfied for the corresponding amplitudes. However, the conditions at $x_2=h$ are replaced with the following one:

$$\left(\bar{\sigma}_{jk}+\sigma_{kn}^{(0)}\frac{\partial \bar{u}_k}{\partial x_n}\right)n_j\Big|_{x_2=h}=p\delta_2^k\quad . \tag{11}$$

In (11), δ_i^j is the Kronecker symbol.

Finally, investigation of the second boundary value problem is reduced to the solution of the boundary value problem given in Eqs. (10), (7), (8) and (11). As noted above, if the right side of the boundary condition in (11) is taken as zero, the boundary value problem (10), (7), (8) and (11) represents the mathematical formulation of the natural vibration problem of the considered plate.

This completes the mathematical formulation of the considered problem.

3 FEM modeling

For the FEM modeling of the boundary value problem in (3)-(5), the functional

$$\Pi^{(0)} = \frac{1}{2}\iiint\limits_{\Omega'} \sigma_{ij}^{(0)}\varepsilon_{ij}^{(0)}d\Omega' + \int\limits_0^h\int\limits_0^{\ell_3} qu_1^{(0)}\Big|_{x_1=0} dx_2dx_3 - \int\limits_0^h\int\limits_0^{\ell_3} qu_1^{(0)}\Big|_{x_1=\ell_1} dx_2dx_3 \tag{12}$$

is used, where Ω' is the solution domain determined by expressions (1) and (2). For the FEM modeling of (10), (7), (8) and (11) the functional

$$\Pi = \frac{1}{2}\iiint\limits_{\Omega'} \left(T_{ij}\frac{\partial \bar{u}_j}{\partial x_i} + \rho\omega^2\bar{u}_i\bar{u}_j\right)d\Omega - \iint\limits_{S_p} T_{ij}n_j\bar{u}_i dS_p \tag{13}$$

is employed, where

$$T_{ij} = \bar{\sigma}_{ij} + \sigma_{ij}^{(0)}\frac{\partial \bar{u}_i}{\partial x_n} \tag{14}$$

In Eq. (14) $\sigma_{ij}^{(0)}$are the component of the initial stresses determined from the solution to the boundary value problem (3)-(5). Employing the well known Ritz technique, we obtain a FEM modeling for each problem from the equations $\delta\prod^{(0)} = 0$ and $\delta\prod = 0$. In these cases, the region Ω' is divided into a certain number of triangular prism finite elements having six corner nodes (for the surroundings of the cylindrical holes) and rectangular prism (brick) elements having eight corner nodes (for the remaining parts of the region not covered by the triangular prism elements) (Fig. 2). The selection of the number degrees of freedom (NDOF) is determined from the requirements that the boundary conditions should be satisfied with very high accuracy and the numerical results obtained for various NDOFs must converge. As is necessary for the finite elements method, the solution domain Ω' is

covered by the finite elements as follows:

$$\Omega' = \bigcup_{k=1}^{M} \Omega'_k \tag{15}$$

where Ω'_k is the region of the k-th finite element (Fig. 2). For the solution procedure, we assume that the unknown values at each node of a finite element are selected displacements only. In other words, we use the displacement-based finite elements for the FEM modeling. (Zienkiewicz and Taylor (1989)).

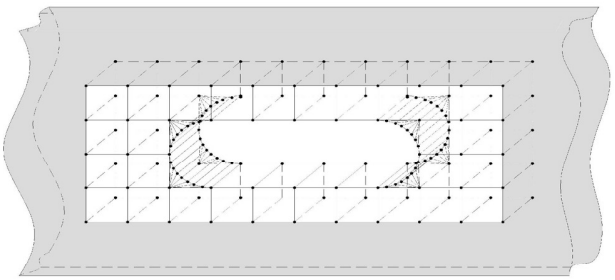

(a)

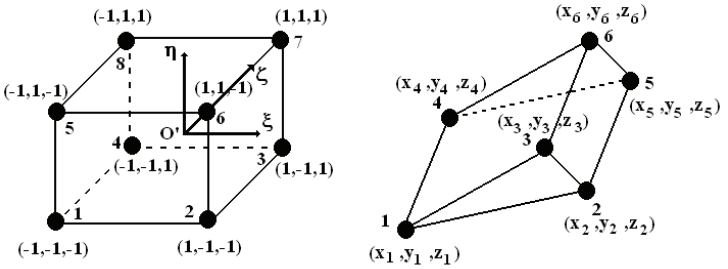

(b)

Figure 2: a) The finite elements mesh around the cylindrical cavity; b) The geometry of the brick and the triangular prism finite elements.

After lengthy mathematical manipulation, the following system of algebraic equations for the first boundary value problem ((3)-(5)) finally yields:

$$\mathbf{K}^{(0)}\mathbf{a}^{(0)} = \mathbf{r}^{(0)} \tag{16}$$

and for the second boundary value problem ((10), (7), (8) and (11))

$$\left(\mathbf{K}-\omega^2\mathbf{M}\right)\mathbf{a}=\mathbf{r} \tag{17}$$

In Eq. (16) and Eq. (17) $\mathbf{K}^{(0)}$ and $\mathbf{K}$ are the stiffness matrices, $\mathbf{M}$ is the mass matrix, $\mathbf{a}^{(0)}$ and $\mathbf{a}$ are the vectors (the components of which are the unknown displacements at the nodes), and $\mathbf{r}^{(0)}$ and $\mathbf{r}$ are the force vectors.

The solutions to Eqs. (16) and (17) give the values of the displacements at each node. However, equation (17) includes the values of the stresses obtained from the solution to the first boundary value problem. So, before finding the solution to Eq. (17) the distribution of stresses for the first boundary value problem should be found. Using the solution to Eq. (16) and Hooke's Law (given in Eq. (3)) they are obtained. The fundamental frequency of the considered plate can be determined from equation:

$$\det\left|\mathbf{K}-\omega^2\mathbf{M}\right|=0 \tag{18}$$

Note that in obtaining the numerical solutions to both of the considered problems, the same number of finite elements is taken and the same arrangements are used for the FEM modeling. The normalized coordinates for the brick finite elements (volume coordinate for the triangular prism finite elements) and Gauss quadrature method are used for the calculation of the numerical integrals with ten sample points in each finite element. We should also note that all computer programs used in the numerical investigations carried out have been composed by the authors in the package FTN77.

4 Numerical results

Assume that the material of the plate is composite consisting of a large number of two different alternating layers. Suppose that the material of each layer is isotropic and that these layers are located on the planes $x_2 = const$. The values related to the matrix and to the reinforcing material will be indicated by the subscripts (1) and (2) respectively; λ_k and μ_k are Lamé constants; E_k is Young's module, ν_k is Poisson's ratio and η_k is the volumetric concentration of the plate's components. Hence, the plate material is transversally isotropic with symmetry axis Ox_2 and the effective mechanical constants A_{ij} in (6) are determined by the expressions given in many references such as Christensen (1979) and Akbarov and Guz (2000).

$$A_{23}=A_{12}=\lambda_1\eta_1+\lambda_2\eta_2-\eta_1\eta_2\left(\lambda_1-\lambda_2\frac{(\lambda_1+2\mu_1)-(\lambda_2+2\mu_2)}{(\lambda_1+2\mu_1)\eta_2+(\lambda_2+2\mu_2)\eta_1}\right),$$

$$\frac{1}{2}(A_{11}+A_{12}) = (\lambda_1+2\mu_1)\eta_1 + (\lambda_2+2\mu_2)\eta_2 - \frac{(\lambda_1-\lambda_2)^2}{(\lambda_1+2\mu_1)\eta_2+(\lambda_2+2\mu_2)\eta_1},$$

$$\frac{1}{2}(A_{11}-A_{13}) = \eta_1\mu_1+\eta_2\mu_2, \quad A_{66}=A_{44}=\frac{\mu_1\mu_2}{\mu_1\eta_2+\mu_2\eta_1}, A_{55}=\eta_1\mu_1+\eta_2\mu_2,$$

$$A_{11}=A_{33},$$

$$A_{22} = (\lambda_1+2\mu_1)\eta_1+(\lambda_2+2\mu_2)\eta_2-\eta_1\eta_2\frac{((\lambda_1+2\mu_1)-(\lambda_1+2\mu_2))^2}{(\lambda_1+2\mu_1)\eta_2+(\lambda_2+2\mu_2)\eta_1} \tag{19}$$

Assume that $\nu_1=\nu_2=0.3, \eta_1=\eta_2=0.5, h/\ell=0.10, \rho_{31}=\ell_3/\ell_1=1$. The geometry of the plate and the considered problem have symmetry with respect to the $x_1=\ell_1/2$ and $x_3=\ell_3/2$ planes. So FEM solutions are obtained in a quarter region. This domain is divided into 30, 12 and 30 brick elements in the direction of the axes Ox_1, Ox_2 and Ox_3 respectively, but 32 triangular prism elements surround the cylindrical hole in a layer. For the FEM modeling 10,200 brick elements, 960 triangular prism finite elements, 13,082 nodes and 37,596 NDOFs were used in total. We introduce the dimensionless parameter $\bar{\omega}^2=\omega^2\rho\ell_1/A_{22}$ through which we estimate the frequency of the additional external forces. First, we calculate the values of the fundamental natural frequency (denoted by $\bar{\omega}_{cr}$) for the problem parameters considered. Moreover, we characterize the magnitude of the initial stretching or compressing force through the parameter q/E_1 and analyze the concentration of the stress in the cylindrical coordinate system $O'r\theta x_3$ (Fig.1).

Note that, before analyzing the numerical results obtained, the algorithm and program coded by the authors and used in the numerical investigations carried out should validate the published results. For this purpose in Table 1 the critical fundamental frequencies are given for various values of the parameter ℓ_3/ℓ_1. It is established that the values $\bar{\omega}^2_{cr}$ decrease with ℓ_3/ℓ_1 and approximate the corresponding values given in Akbarov and Guz (2000) obtained from the plane strain-state.

The values given in Table 2 show the effect of the volume of the cylindrical holes and the initial stretching force on $\bar{\omega}^2_{cr}$. These numerical results show that the values of $\bar{\omega}^2_{cr}$ approximate a certain asymptote with a decrease in the volume of the hole i.e. with a decreasing ratio in V_h/V. The value of this asymptote is the value of $\bar{\omega}^2_{cr}$ for the corresponding plate without a hole (Akbarov and Guz, (2000)). Based on these observations, the reliability and validation of the programs and coded algorithms are verified.

In Table 3 the values of $\bar{\omega}^2_{cr}$ of the considered plate for various q/E_1 and E_2/E_1 for which $h/\ell_1=0.10$; $c/R=11$; $V_h/V=4.8854*10^{-2}$ and $R/\ell_1=8.3333*10^{-3}$ are

Table 1: The effect of ℓ_3/ℓ_1 on $\bar{\omega}_{cr}^2$ for the rectangular plate without cylindrical cavities ($h/l_1 = 0.1$).

E_2/E_1	ℓ_3/ℓ_1				Akbarov and Guz (2000)
	1	2	3	4	
1	0.23	0.09	0.08	0.07	0.06
10	0.56	0.24	0.21	0.19	-
20	0.93	0.41	0.35	0.33	0.31
50	1.92	0.80	0.70	0.67	0.62

Table 2: The values of $\bar{\omega}_{cr}^2$ for various V_h/V (Total volume of two cavities/Volume of the plate without cavities) in the case where$h/l_1 = 0.1, l_3/l_1 = 1, h_A = h_U = 5R, R = H/12$ and $c/R = 11$.

$\frac{q}{E_1}$	$\frac{E_2}{E_1}$	$10^2 * V_h/V$				
		6.1770	4.8854	3.5937	1.6562	0
0	1	0.271	0.259	0.249	0.239	0.238
	10	0.634	0.607	0.586	0.567	0.566
0.001	1	0.285	0.274	0.263	0.250	0.245
	10	0.643	0.617	0.594	0.572	0.570
0.005	1	0.339	0.334	0.317	0.297	0.274
	10	0.680	0.654	0.628	0.598	0.586

Table 3: The values of $\bar{\omega}_{cr}^2$ of the considered plate for various q/E_1 and E_2/E_1 for which $h/l_1 = 0.10$; $c/R = 11$; $V_h/V = 4.8854 \times 10^{-2}$ and $R/l_1 = 8.3333 \times 10^{-3}$.

q/E_1	E_2/E_1		
	1	5	10
-0.01	0.096	0.299	0.510
-0.005	0.179	0.351	0.559
-0.001	0.243	0.392	0.597
0	0.259	0.403	0.607
0.001	0.274	0.413	0.617
0.005	0.334	0.453	0.654
0.01	0.407	0.503	0.701

given. The numerical results given in Table 3 show that the values of $\bar{\omega}_{cr}^2$ increase with E_2/E_1. It is concluded that an increase in the absolute values of q/E_1 causes an increase (a decrease) in the values of $\bar{\omega}_{cr}^2$ under initial stretching (under initial

compressing).

Table 4: The values of $\bar{\omega}_{cr}^2$ of the considered plate for various q/E_1, E_2/E_1 and c/R for which $h/l_1 = 0.10$; $c/R = 11$; $V_h/V = 4.8854 \times 10^{-2}$ and $R/l_1 = 8.3333 \times 10^{-3}$.

q/E_1	E_2/E_1	c/R				
		6.5	11	15.5	20	42.5
0	1	0.255	0.259	0.263	0.267	0.308
	5	0.397	0.403	0.409	0.416	0.482
	10	0.600	0.607	0.616	0.626	0.717
0.005	1	0.319	0.334	0.334	0.342	0.383
	5	0.441	0.453	0.458	0.468	0.534
	10	0.642	0.654	0.662	0.675	0.768

In Table 4 the values of $\bar{\omega}_{cr}^2$ of the considered plate for various q/E_1, $E_2/E_1$and c/R for which $h/\ell_1 = 0.10$; $V_h/V = 4.8854 * 10^{-2}$ and $R/\ell_1 = 8.3333 * 10^{-3}$ are given. The numerical results given in this table show that the values of $\bar{\omega}_{cr}^2$ increase with c/R. This means that if the distance between the two neighboring cylindrical cavities decreases, i.e. the two cavities are close to each other, the fundamental frequency $\bar{\omega}_{cr}^2$decreases. Table 4 also shows that the initial stretching forces cause an increase in the values of $\bar{\omega}_{cr}^2$.

Table 5: The values of $\bar{\omega}_{cr}^2$ of the considered plate for various q/E_1, E_2/E_1 and h_U/R for which $h/l_1 = 0.10$; $c/R = 11$; $V_h/V = 4.8854 \times 10^{-2}$ and $R/l_1 = 8.3333 \times 10^{-3}$.

q/E_1	E_2/E_1	h_U/R			
		5	4	3	2
0	1	0.259	0.258	0.255	0.249
	5	0.403	0.401	0.395	0.385
	10	0.607	0.604	0.595	0.579
0.005	1	0.334	0.298	0.253	0.188
	5	0.453	0.434	0.409	0.371
	10	0.654	0.640	0.617	0.580

In Table 5 the values of $\bar{\omega}_{cr}^2$ of the considered plate for various q/E_1, $E_2/E_1$and H_U/R for which $h/\ell_1 = 0.10$, $V_h/V = 4.8854 * 10^{-2}$ and $R/\ell_1 = 8.3333 * 10^{-3}$ are given. The numerical results given in Table 5 show that the values of h_U/R, i.e. the distance between the cavity and the upper free face plane of the rectangular

plate, significantly affect the values of $\bar{\omega}_{cr}^2$. Hence, the values of $\bar{\omega}_{cr}^2$ decrease with a decrease in the values of h_U/R.

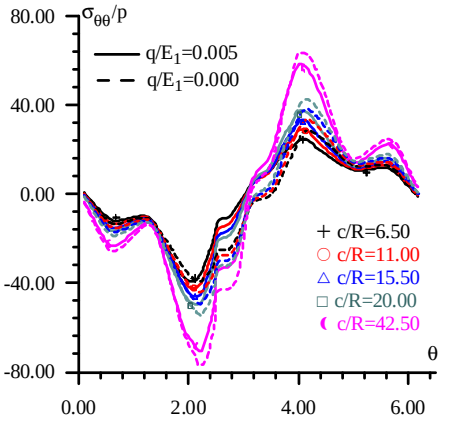

Figure 3: The influence of the distance between two cavities (c/R) on the values of $\sigma_{\theta\theta}/p$ with respect to θ for the case where E_2/E_1 and $\bar{\omega}^2 = 0.16$.

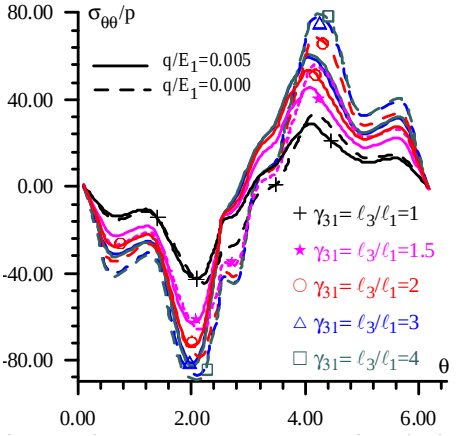

Figure 4: The influence of $\gamma_{31} = l_3/l_1$ on the values of $\sigma_{\theta\theta}/p$ for the case where $E_2/E_1 = 10, \bar{\omega}^2 = 0.16$ and $c/R = 11$.

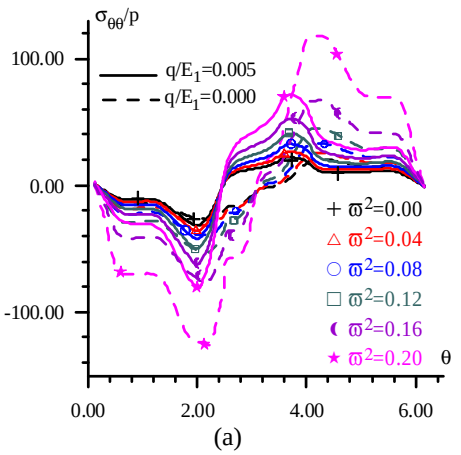

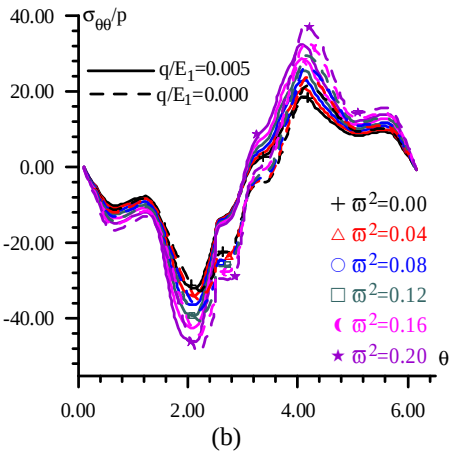

Figure 5: The influence of $\bar{\omega}^2$ on the values of $\sigma_{\theta\theta}/p$ for the case where $c/R = 11$ a) For $E_2/E_1 = 1$, b) For $E_2/E_1 = 10$

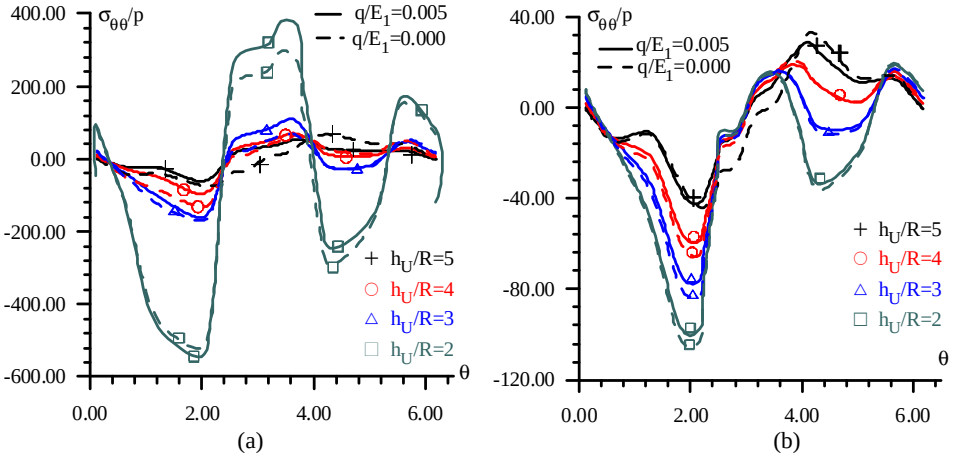

Figure 6: The influence of h_U on the values of $\sigma_{\theta\theta}/p$ for the case where $\bar{\omega}^2$ and $c/R = 11$ a) For $E_2/E_1 = 1$, b) For $E_2/E_1 = 10$

Figure 3 shows the influence of the distance between the cavities (c/R) on the values of $\sigma_{\theta\theta}/p$ with respect to θ around the left cylindrical cavity at the mid-point of each element on the cross section $x_3/\ell_3 = 0.5$ for $\bar{\omega}^2 = 0.16$, $h/\ell_1 = 0.10$; $h_U/R = 5$; $E_2/E_1 = 10$; $V_H/V = 4.8854 * 10^{-2}$ and $R/\ell_1 = 8.3333 * 10^{-3}$. It follows from the graphs that the absolute local maximal values of $\sigma_{\theta\theta}/p$ increase monotonically with increasing c/R for the cases where $q/E_1 \neq 0$ and $q/E_1 = 0$.

Figure 4 shows the influence of $\gamma_{31} = \ell_3/\ell_1$ on the values of $\sigma_{\theta\theta}/p$ for the case where $E_2/E_1 = 10, \bar{\omega}^2 = 0.16$ and $c/R = 11$. $\gamma_{31} = \ell_3/\ell_1$ represents the ratio of the lengths along the two perpendicular directions, i.e. the length of the plate along the Ox_3 axis (denoted by ℓ_3) and along the Ox_1 axis (denoted by ℓ_1). It follows from the graphs that the absolute values of $\sigma_{\theta\theta}/p$ increase monotonically with increasing $\gamma_{31} = \ell_3/\ell_1$ for the cases where $q/E_1 \neq 0$ and $q/E_1 = 0$, and approach a certain limit value, i.e. the value which is determined from the corresponding boundary-value problem related to the corresponding plane-strain state. These results also confirm the reliability of the algorithm and the PC programs composed by the authors and used for determination of the numerical solution.

Figure 5 shows the influence of the dimensionless frequency $\bar{\omega}^2$ on the values of $\sigma_{\theta\theta}/p$ where $h/\ell_1 = 0.10$, $h_U/R = 5$, $V_h/V = 4.8854 * 10^{-2}$, $R/\ell_1 = 8.3333 * 10^{-3}$ for $E_2/E_1 = 1$ (Fig. 5a) and $E_2/E_1 = 10$ (Fig. 5b). It follows from the graphs that the absolute values of $\sigma_{\theta\theta}/p$ increase monotonically with $\bar{\omega}^2$.

Figure 6 shows the influence of the upwards replacement of the position of the

cavities (i.e. the influence of the parameter h_U/R) on the values of $\sigma_{\theta\theta}/p$ for the case where $h/\ell = 0.10$, $V_h/V = 4.8854 * 10^{-2}$, $h_A/R = h/R - h_U/R$ and $R/\ell_1 = 8.3333 * 10^{-3}$. It follows from the graphs that the absolute values of $\sigma_{\theta\theta}/p$ increase monotonically with decreasing h_U/R for the cases where $q/E_1 \neq 0$ and $q/E_1 = 0$.

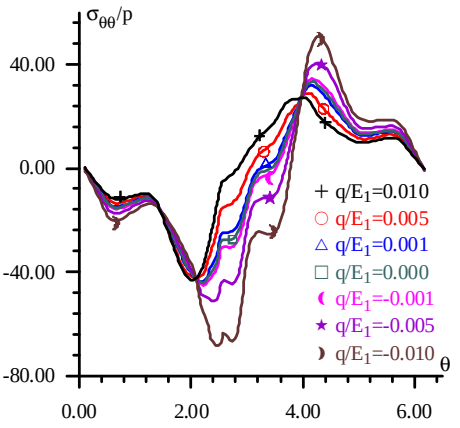

Figure 7: The influence of q/E_1 on the values of $\sigma_{\theta\theta}/p$ for the case where $E_2/E_1 = 10$, $\bar{\omega}^2 = 0.16$ and $c/R = 11$.

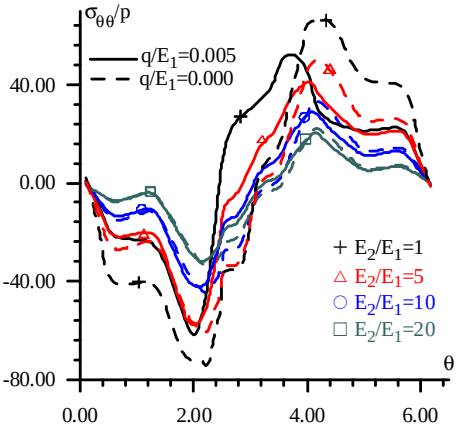

Figure 8: The influence of E_2/E_1 on the values of $\sigma_{\theta\theta}/p$ for the case where $E_2/E_1 = 10$, $\bar{\omega}^2 = 0.16$ and $c/R = 11$.

Figure 7 shows the influence of the initial force, i.e. of q/E_1, on the values of $\sigma_{\theta\theta}/p$ calculated for the case where $h/\ell_1 = 0.10$, $h_U/R = 5$, $E_2/E_1 = 10$, $V_h/V = 4,8854 * 10^{-2}$ and $R/\ell_1 = 8.3333 * 10^{-3}$. In obtaining these results, the case where $q/E_1 > 0$ ($q/E_1 < 0$) is taken as the case where the initial forces are stretching (compressing) ones. It follows from the graphs that the distributions of $\sigma_{\theta\theta}/p$ obtained under the initial stretching (compressing) are completely shifted compared with the graph obtained for the case where the initial force is absent i.e. $q/E_1 = 0$. However, an increase in the absolute values of q/E_1 under initial tension (compression) causes a decrease (an increase) in the local absolute maximums values of the stress $\sigma_{\theta\theta}/p$.

Figure 8 shows the influence of E_2/E_1 on the values of $\sigma_{\theta\theta}/p$ for $h/\ell_1 = 0.10$, $h_U/R = h_A/R = 5$ and $R/\ell_1 = 8.3333 * 10^{-3}$. It follows from the graphs that the absolute values of $\sigma_{\theta\theta}/p$ decrease monotonically withE_2/E_1.

5 5 Conclusion

Based on the discussions in this paper, the following conclusions can be drawn:

- The values of the fundamental frequency $\bar{\omega}^2_{cr}$ approximate a certain asymp-

tote with a decrease in the total volume of the cavities i.e. with a decrease in the ratio of V_h/V.

- The value of this asymptote is the value of $\bar{\omega}_{cr}^2$ for the corresponding plate without cavities.
- The values of the fundamental frequency $\bar{\omega}_{cr}^2$ increase (decrease) with the initial stretching (compressing) force i.e. with absolute values of q/E_1.
- The values of the fundamental frequency $\bar{\omega}_{cr}^2$ increase with the distance between the cavities.
- The values of the fundamental frequency $\bar{\omega}_{cr}^2$decrease as these cavities approach the upper free face plane of the plate i.e. with a decrease in the values of h_U/R.
- The stress concentration of $|\sigma_{\theta\theta}|/p$ around the cavities increases monotonically with the distance between the cavities.
- An increase in the values of the frequency of the external forces causes an increase in the values of $|\sigma_{\theta\theta}|/p$.
- The influence of the initial stresses in the plate on the dynamic (time-harmonic) stress concentration $|\sigma_{\theta\theta}|/p$ becomes more significant with a decrease in the value of h_U/R.
- The stress concentration of $|\sigma_{\theta\theta}|/p$ around the cavities decreases (increases) with the stretching (compressing) forces i.e. with q/E_1.
- The stress concentration of $|\sigma_{\theta\theta}|/p$ which appears around the holes increases monotonically with $\gamma_{31} = \ell_3/\ell_1$ and approaches a certain limit value, i.e. the value is determined from the corresponding boundary-value problem in the plane-strain state. At the same time, this concentration decreases with E_2/E_1.

References

Akbarov S. D.; Guz A.N. (2000): *Mechanics of Curved Composites*, Dordrecht, The Netherlands, Kluwer.

Akbarov S.D.; Yahnioglu N.; Babuscu Yesil U. (2008): *Interaction Between Two Neighbouring Circular Holes in a Pre-Stretched Simply Supported Orthotropic Strip Under Bending*, Mechanics of Composite Materials, vol. 44, No. 6, pp.827-838.

Akbarov S.D.; Yahnioglu N.; Babuscu Yesil U. (2010): *Forced Vibration Of An Initially Stressed Thick Rectangular Plate Made of an Orthotropic Material With A Cylindrical Hole, Mechanics of Composite Materials*, vol. 46, no. 3, pp. 287-298.

Akbarov, S. D., Yahnioglu, N., Yucel, A.M. (2004): On the influence of the initial tension of a strip with a rectangular hole on the stress concentration caused by additional loading. J. Strain Analysis, 39(6), 615-624.

Babuscu Yesil U. (2010): *The Effect of the Initial Stretching of The Rectangular Plate With a Cylindrical Hole on The Stress and Displacement Distributions Around The Hole*, Turkish J. Eng. Env. Sci., vol. 34, pp. 1-15.

Chaudhuri, R. A. (2007): *Weakening Effects of Internal Part-Through Elliptic Holes in Homogeneous and Laminated Composite Plates*, Composites Structures, vol. 81, pp. 362-373.

Chernopiskii, D. I. (2009): *Convergence of solutions for noncanonical bodies found by the boundary-shape perturbation method*, International Applied Mechanics, vol. 45, No. 8, pp. 882-887.

Christensen, R.M. (1979): *Mechanics of Composite Materials*, John Willey and Sons, Int. New York.

Guz, A.N. (2004): Elastic waves in bodies with initial (residual) stresses. "A.C.K.", Kiev.

Khoma I. Y.; Kondratenko, O. A. (2008): *Stress distribution around a circular cylindrical cavity in a prestressed plate*, International Applied Mechanics, vol. 44, No. 1, pp. 23-33.

Kwaka M. K.; Han S. (2007): *Free vibration analysis of rectangular plate with a hole by means of independent coordinate, coupling method*, Journal of Sound and Vibration, vol. 306, pp. 12–30.

Savin, G. N. (1961): Stress *Concentration Around Holes*, E. Gros Translator, Pergomon.

Sivakumar K.; Iyengar N. G. R. (1999): *Free vibration of laminated Composite plates with cutout*, Journal of Sound and Vibration,vol. 221, No. 3, pp. 443-470.

Toubal, L.; Karama, M.; Lorrai B. (2005): *Stress concentration in a circular hole in composite plate*, Composite Structures, vol 68, no.1, pp. 31-36.

Yahnioglu N. (2007): *On the Stress Distribution in the Pre-Stretched Simply Supported Strip Containing Two Neighbouring Circular Holes Under Forced Vibration*, International Applied Mechanics, vol. 43**,** No. 10, pp. 135-140.

Yahnioglu N.; Babuscu Yesil U. (2009): *Forced vibration of an initial stressed rectangular composite thick plate with a cylindrical hole*, ASME 2009 International Mechanical Engineering Congress and Exposition IMECE09 November 13-

19, 2009, Lake Buena Vista, Florida, USA.

Zamanov, A.D. (1999): *On The Stress Distribution in a Rectangular Thick Plate of a Composite Material With Curved Structure Under Forced Vibration*, Mechanics Of Composite Materials, vol. 35, No. 4, pp. 301-336.

Zhen, W.; Wanji C. (2009): *Stress analysis of laminated composite plates with a circular hole according to a single-layer higher-order model*, Composite Structures, vol. 90, pp.122–129.

Zheng Y.; Chang-Boo K.; Chongdu C.; Hyeon G. B. (2008): *The concentration of stress and strain in finite thickness elastic plate containing a circular hole*, International Journal of Solids and Structures, vol.45, no.3-4, pp.713-731.

Zienkiewicz O.C.; Taylor R.L. (1989): *The Finite Element Methods: Basic Formulation and Linear Problems*, vol. 1, 4^{th}Ed., Mc Graw-Hill Book Company, Oxford.